Original article

Synergistic enhancement of cellular uptake with CD44-expressing malignant pleural mesothelioma by combining cationic liposome and hyaluronic acid-lipid conjugate

Yu Sakurai[a,*], Akari Kato[a], Yasuhiro Hida[b], Junichi Hamada[c], Nako Maishi[d], Kyoko Hida[d], Hideyoshi Harashima[a,*]

[a]Faculty of Pharmaceutical Sciences, Hokkaido University, Sapporo 060-0812, Japan

[b]Department of Cardiovascular and Thoracic Surgery, Graduate School of Medicine, Hokkaido University, Sapporo 060-8638, Japan;

[c]Health Sciences University of Hokkaido, School of Nursing and Social Services, Tobetsu-cho 061-1852, Japan

[d]Vascular Biology and Molecular Pathology, Graduate School of Dental Medicine, Hokkaido University, Sapporo 060-8586, Japan

*Co-corresponding authors

Correspondence should be addressed to Hideyoshi Harashima (harasima@pharm.hokudai.ac.jp) or Yu Sakurai (yu-m@pharm.hokudai.ac.jp)

Kita-12, Nishi-6, Kita-ku, Sapporo 060-0812, Japan.

TEL: +81-11-706-3919, FAX: +81-11-706-4879

Abstract

Malignant pleural mesothelioma (MPM) is a highly aggressive form of cancer, with a median survival of less than one year. It is well known that the hyaluronan (HA) receptor CD44 is highly expressed by MPM cells and is reported to be correlated with a poor prognosis. We herein report on the development of a new type if drug delivery system against CD44 that involves the use of lipid nanoparticles (LNPs) equipped with a new type of HA derivative. In this study, we evaluated HA-lipid conjugation (HAL) via the end of the HA molecule through reductive amination, a process that allowed the carboxylate group to remain intact. As a result, the HAL-modified LNP appears to be a potent nanoparticle for dealing with MPM. Surprisingly, the use of a combination of a cationic lipid and HAL had a synergistic effect on cellular uptake in MPM and consequently permitted an anti-cancer drug such as cis-diamminedichloro-platinum(II) (CDDP). Intrapleural injection of CDDP-loaded HAL-LNP (1.5 mg/kg as CDDP) per week significantly suppressed the progression of this type of cancer in a MPM orthotopic model. These results suggest that HAL-modified LNP represents a potent delivery system for MPM cells that express high levels of CD44.

Keyword: lipid nanoparticle, hyaluronan, CD44, malignant pleural mesothelioma

1. Introduction

Malignant pleural mesothelioma (MPM) is a rare, but aggressive form of cancer, that originates in mesothelial cells of the pleura. MPM is mainly caused by a long exposure (typically 30-40 years) to asbestos.[1] While the disease is predicted to peak in approximately 2025 in the EU, Australian and Japan.[2,3], asbestos is still consumed in developing Asian countries[4] In addition, the median survival is 9 to 12 months from the first diagnosis.[5] Given these facts, developing an innovative therapy for MPM has become an urgent issue.

Several therapies, including, chometherapy, surgery and radiation therapy have been explored for MPM patients. Historically, extra-plural pneumonectomy (EPP) or extended pleurectomy decortication (EPD) was frequently performed on MPM patients. However, in the American Society of Clinical Oncology (ASCO), such only surgical resections of solid tumor is not recommended due to the high risk and difficulty associated with operation, plus the fact that these procedures are largely insufficient.[6] Instead, they recommend multimodal therapy, for example surgery with pre- or post-chemotherapy (neo-adjuvant or adjuvant). The latest studies revealed that a combination therapy involving an anti-vascular endothelial cell growth factor (VEGF)-A antibody (bevacizumab) and an immune checkpoint inhibitory antibody against programmed cell death (PD)-1 (nivolumab) and PD-L1 (ipilimumab) in addition of surgery and neo-adjuvant therapy can significantly improve clinical outcomes for MPM patients.[7-10]

Although the chemotherapy plays an important role in MPM treatment, the response ratio of even the currently most popular regimen for MPM (cis-diamminedichloro-platinum(II) (CDDP)-pemetrexed combined chemotherapy) is only 41.3%.[11] Despite a large extent of progress in therapy for MPM, clinical outcome is significant, but limited

and there is no second line treatment.[12,13] Therefore, a more effective type of chemotherapy would be required for the treatment of MPM patients.

To efficiently deliver therapeutics, such as small molecules and nucleic acids, we recently developed a series of actively targeting-type lipid nanoparticles (LNPs), which are equipped with a ligand that specifically recognizes target cells using peptides and biomolecules.[14-17] Such ligand-equipped LNPs can specifically deliver them to cancer cells and are highly selective for specific target cells and consequently circumvent adverse effects derived from the unintended accumulation of anti-cancer therapeutics in off-target organs.[18,19] Thus, targeted-LNPs have shown prominent therapeutic outcomes in a mouse model.[20] To target MPM, we focused on hyaluronan (HA) as a specific ligand. Hyaluronan is a negatively charged polysaccharide comprised of N-acetylglucosamine (GlcNAc) and glucuronic acid (GlcUA) units.[21] CD44 is a well-known receptor for HA[22,23] Although a high expression level of CD44 is known to occur in a wide range of cancers,[24] CD44 expression is significantly relevant to the diagnosis and prognosis of MPM.[25,26] It therefore appears that HA would be a potent ligand for targeting MPM.

A number of groups have reported on the use of HA-decorated LNPs for targeting cancer cells that express high levels of CD44. The modification of LNPs with HA follows two possible pathways; electrostatic interaction and covalent bond formation via the carboxylic acid groups in HA. To associate LNPs with negatively charged HA, cationic lipids, such as 1,2-dioleoyl-3-trimethylammoniumpropane (DOTAP), are used. Typically, the prepared cationic LNPs are simply incubated in a HA solution in order to coat the LNPs with HA.[27,28] In the other route, prepared LNPs containing lipids with primary amine are incubated with HA in the presence of carbodiimide and N-hydroxysuccinimide to form an amide bond between the amine group and the carboxylate group in HA.[29-32] In both

cases, the carboxylic acid group in HA is utilized to develop non-covalent or covalent binding. In a previous report, however, an X-ray crystal structure analysis of an HA-CD44 complex indicated that the oxygen atoms of the carboxylic acid groups in HA were associated with Ala102, Ala103 and Tyr83, which play a key role in the recognition process.[33] To circumvent this interaction via carboxylate groups, we designed HA-derivatives that are conjugated to the lipid through reductive amination at the reducing end of the HA molecule (HAL). We then optimized the resulting HAL-containing LNPs in terms of intracellular uptake and delivery efficiency to target MPM cells that express high levels of HA in an *in vivo* model mouse.

2. Materials and Methods

2.1 Materials

HA (MW 50,000) was generously provided by the Kewpie Corporation. Distearoyl-*sn*-glycerophosphoethanolamine (DSPE), 1-Stearoyl-2-oleoyl-*sn*-glycerophosphoethanolamine (SOPE), Dioleoyl-*sn*-glycerolphosphoethanolamine (DOPE) and poly(ethyleneglycol) (PEG)2000-DSPE were purchased from NOF Corporation (Tokyo, Japan). DOTAP, 1,2-distearoyl-3-trimethylammoniumpropane (DSTAP) and dimethyldioctadecylammonium (DDAB) were purchased from Avanti Polar Lipids (Alabaster, AL, USA). The WST-8 reagent was obtained from Dojindo (Kumamoto, Japan). 3,3-Dioctadecyloxacarbocyanine perchlorate (DiO) and 1,1'-dioctadecyl-3,3,3',3'- tetramethylindodicarbocyanine (DiD) were purchased from PromoKine (Heidelberg, Germany). Cholesteryl 3β-N-(di-methyl-amino-ethyl)-carbamate hydrochloride (DC-chol) was obtained from Sigma-Aldrich (St. Louis, MO, USA). Cis-diamminedichloro-platinum(II) (CDDP) and DMEM/Ham's F-12 medium were purchased from Wako Pure Chemical Industries (Osaka, Japan). All other chemicals used were commercially available reagent-grade products.

2.2 Synthesis of hyaluronic acid – lipid conjugate (HAL)

The conjugation of lipid to HA was carried out according to a previous report as shown in Fig. 1.[34] Typically, HA (0.10 mmol) was stirred in a solution of 100 mL of dry dimethyl sulfoxide (DMSO) and 10 mL of acetic acid at 60 °C for 2 hours. Triacetoxyborohydride (0.40 mmol, 4 equiv.) was then gradually added to the mixture over a period of 40 min after the addition of phosphoethanolamine (0.20 mmol, 2 equiv.). The mixture was stirred for 96 hours, and

the solvent was then removed at 100 °C *in vacuo*. The crude product was purified by reverse-phase liquid chromatography (gradient water/MeOH), and the solvent was then removed by freeze-drying. The degree of conjugation was evaluated by calculating integration ratio of acetyl group (hyaluronan) and methylene group by ^{1}H nucleic magnetic resonance.

2.2. Cell culture

H226 cells were obtained from the American Type Culture Collection. HMM1 and HMM3 were established from one patient (57-year-old) and the other (65-year-old) as previously reported.[35,36] Cells were maintained in DMEM/Ham's F-12 medium supplemented with 10% fetal bovine serum and 100U/mL penicillin and 100 μg/mL streptomycin under a 5% CO_2 atmosphere.

2.3. Evaluating expression of hyaluronan receptor

After trypsinizing the cells, they were seeded on 6-well plates at a density of 1.0×10^5 cells/well. Cells were treated with Alexa Fluor 647-anti-mouse/human CD44 antibody (Biolegend, San Diego, CA, U.S.A., 103008) for 30 min on ice. After washing the cells twice with phosphate-buffered saline without Mg^{2+} nor Ca^{2+} (PBS (−)) containing 1.0% bovine serum albumin and 0.05% NaN_3, they were analyzed with a flow cytometer Gallios (Tokyo, Japan)

2.4. LNP preparation

The lipids in ethanol (total 4,000 nmol) were first added to a glass tube at indicated lipid ratio and the solvent

was then removed by a stream of N_2 gas. The lipid thin layer was hydrated by 1.5 mL of PBS (−), and sonicated using a bath-type sonicator for 30 sec. The obtained LNP was then processed through an Extruder (Avanti Polar Lipids). HA or HAL was incorporated into the LNPs by incubating them with HA or HAL in 10% ethanol for 30 min at 60° C at 0.5 mol% to 2.0 mol% against total lipid amount. To encapsulate CDDP, CDDP was dissolved at 3 mg/mL in PBS (−) by heating, and then used at the hydration step. Unencapsulated CDDP was removed by Amicon Ultra-15 filtration (Merck-Millipore, Darmstadt, Germany). The recovery ratio of CDDP was measured by inductively Coupled Plasma – Atomic Emission Spectrometry (ICP-AES) ICPE-9000 (Shimadzu, Kyoto, Japan). Standard curve was plotted by sequential dilution of 1.0 mg/mL CDDP Standard solution.

2.5. Cell viability assay

The CDDP-loaded LNP was added to cells at 0.1 – 20 μg/mL of CDDP 24 hours after the cells had been seeded in a 96-well plate at a density of 1.0×10^4 cells/well. At twenty-four hours after the addition, 10 μL of WST-8 reagent in 90 μL of DMEM/Ham's/F12 were added to wells and the suspension then incubated for 1 hour. The absorbance of the culture medium was measured at 450 nm with a plate reader Infinite M200 (Tecan, Männedorf, Switzerland). Cell viability was calculated by setting the non-treated cells as 100% viable.

2.6. Analysis of in vivo distribution and therapeutic effect of intrapleural injected LNPs.

To label LNPs with a radio isotope (RI), approximately 1,000,000 dpm of [^{3}H]-cholesteryl hexadecyl ether was added to the lipid mixture. The RI-labeled LNPs were intrapleurally administered to the MPM model mouse mice.

The MPM model mice were intrapleurally inoculated with 1.0×10^7 H226 cells. Cancer, lung, heart, kidney, liver and spleen tissues were collected at 24 hours after the injection, and were dissolved in 2 mL of Soluene-350 (PerkinElmer, Waltham, MA, USA). Hionic-Fluor (20 mL) was added to the dissolved organ solution at 55°C. After storing the solutions overnight, the radio activity was measured by a, LSC6100 scintillation counter (Hitachi-Aloka Medical, Tokyo, Japan).

For an evaluation of therapeutic effect of CDDP-loading HAL-LNP, MPM-bearing athymic mice were treated 4 times per week with 1.5 mg/kg HAL-LNP as the CDDP dosage. The progression of MPM was visually evaluated 45 days after the inoculation.

2.7. Statistical Analysis

The Student's t-test was carried out for pairwise comparison. For comparison among three or more groups, non-repeated analysis of variance (nrANOVA), followed by Bonferroni test or SNK test. P value < 0.05 was regarded as a statistically significant difference. Interaction effects were analyzed by Two-way ANOVA using the SigmaPlot software.

3. Results & Discussion

3.1 Optimization of HAL-modified LNPs with CD44-positive MPM cells

In initial experiments, CD44 expression in 3 cell lines of MPM cells was evaluated by flow cytometry. The results indicated that the HMM3 and H226 cells expressed high levels of CD44 and the HMM1 expressed moderate levels (Fig. 2). The HMM3 and H226 cells were subsequently used as CD44 positive cell lines, while HMM1 cells were used as a CD44 negative cell line. We then investigated the effect of HA and HAL on the cellular uptake of LNP. In previous reports, LNP was modified with HA by electrostatic interaction between cationic LNP and anionic HA molecules [21,37,38]. Data on the characterization of these carriers are shown in Table 1. The inversion of Z-potential from positive to negative indicates that HA was successfully associated with the surface of the LNPs. On the other hand, the diameter of the LNPs was not changed substantially as the result of the HA modification. Despite the previous reports on the success with simply coating HA on an LPN, the cellular uptake of such a HA/cationic LNP complex did not increase, at least in MPM cells (Fig. 3A and 3B). Previous study involving computational simulations revealed that the carboxylic acid group in HA is important for successfully achieving an interaction between HA and CD44.[33] This explains why, when a carboxylic acid group is utilized to achieve an interaction between nanoparticles and HA, an enhancement in cellular uptake might not be observed. On the other hand, modification of the HA-lipid conjugate with HAL significantly enhanced the uptake of the cationic liposome, but not the neutral liposome in both cell lines (Fig. 4A and B). It is noteworthy that the characterization of the HA/LNP and HAL-LNP was not significantly different as shown in Table 2. Synergistic interactions between the cationic lipid DOTAP and HAL was observed within 10 mol% of DOTAP, which was statistically significant by a two-way ANOVA test, but not 15 mol%.

Previous reports also showed that the combination of a cationic peptide and a specific ligand had a synergistic effect on cellular uptake.[18,39] In addition, Xia QS *et al.* (in a computational analysis) reported that nanoparticles with two ligands were synergistically taken up by cells through unknown mechanisms.[40] It is speculated that cationic component would facilitate endocytosis after approaching target cells through interaction between HA and CD44. However, the underlying mechanisms for synergistic uptake have been unveiled yet. Further studies should be required for an elucidation of such synergistic uptake mechanism. In this study, the incorporation of 10 mol% cationic lipids into the HAL-modified LNP was regarded as the optimum condition.

To investigate which cationic lipid was the most efficacious for synergistically improving the cellular uptake of the HAL-conjugated LNP, 4 commercially available cationic lipids (DOTAP, DSTAP, DDAB, DC-chol) were incorporated into lipid envelope of HAL-LNP. In both H226 and HMM3, a similar enhanced uptake was observed (Fig. 5A). Consequently, we used HAL-modified LNP that contained DOTAP in subsequent experiments. The optimum density of HAL was next examined. Cellular uptake was evaluated by flow cytometry for a preparation of HAL containing 0.5 ~ 6.0 mol% total lipid, As shown in Fig. 5B, the highest cellular uptake was observed when 2.0 mol% of HAL was incorporated into the LNP. Therefore, 2.0 mol% of HAL modification was considered to be the optimum concentration. The cellular uptake of the HAL-conjugated LNP in HMM3 cells was lower than that in H226 cells. This can be attributed to the relatively lower expression of CD44 in HMM3 cells than that in H226 cells. Then, we evaluated the cellular uptake of HAL-LNP after the addition of free HA (10 mg/mL). As shown in Supplemental Figure 1, the cellular uptake of HAL-LNP was moderately inhibited. However, as medium was too viscous in the presence of over 10 mg/mL of HA, we didn't evaluate the inhibitory effect of free HA at higher concentration. These

results suggest that the HAL-modified LNP is an efficient, selective system for delivery to CD44 cells.

3.2 Evaluation of in vitro pharmacological effects

To confirm whether the LNP simply becomes attached to the cell surface or if it actually enters the cytosol, CLSM images was observed after the addition of DiI labeled LNP (Fig. 6). When the non modified LNP was added to H226 cells, a small amount of LNP was taken up by cells. On the other hand, HAL-LNP was observed throughout the cells, including the perinucleus.

To evaluate the therapeutic effect of HAL-LNP, CDDP was used as a cytotoxic reagent. CDDP was encapsulated by the lipid thin layer method because CDDP is currently used as a standard therapy for the treatment of MPM.[41] The recovery ratio of CDDP in the LNP particles was 1.51 ± 0.50 % (151.9 ± 41.6 μg/mL). The characterization of HAL-LNP loading-CDDP was performed by a ZetaSizer. The diameter of HAL-LNP was 262 ± 29 nm, zeta-potential was -36 ± 3 mV. The CDDP-loaded HAL-LNP was equal to the free CDDP in terms of cell killing activity, which was approximately 2-fold lower than that for the CDDP-loaded LNP (Fig. 7). The encapsulation of anti-cancer therapeutics into PEGylated nanoparticles generally decreases the overall cell killing effect, perhaps because of weakened cellular uptake and endosomal escape. [42-44] Whereas, the HAL-LNP with encapsulated CDDP was superior to free CDDP, specifically in CD44-high H226 cells. These observations indicate that HAL-modification of a cationic LNP has the potential to deliver therapeutics to CD44-positive MPM cells.

3.3 Evaluation of in vivo accumulation in the MPM model via intrapleural injection

Currently, a number of clinical studies on local chemotherapy via the intrapleural injection of anti-cancer agents, such as CDDP, after the surgery are underway, because the toxicity of the intrapleural injection of the therapeutics is more tolerable than that of the systemic injection because less drug leaks into the circulation.[45-47] Accordingly, we used the intrapleural injection of HAL-LNP as the route of administration. To evaluate the issue of whether the HAL-LNP is applicable for in vivo experiments, the accumulation of the preparation in lung, heart, kidney, liver, spleen and tumor at 24 hours after the left intrapleural injection of RI-labeled LNP and HAL-LNP was measured (Fig. 8A). Concerning the tumor, HAL-LNP tended to accumulate in tumor tissue more heavily compared to LNP (13.5 ± 10.2 %ID/organ vs. 23.2 ± 7.8 %ID/organ). On the other hand, the amount of LNP that accumulated in lung and liver was higher than that of the HAL-LNP. In addition, the extent of leakage in the blood from the pleural cavity for the HAL-LNP was just 3.1 ± 1.2 %ID/mL blood. These results suggest that the pleural injection of HAL-LNP could induce an adverse effect against normal tissues because of the low leakage to the blood circulation and subsequent accumulation in normal tissues. We also observed the accumulation of HAL-LNP in the lung and heart, which are in close proximity to the MPM solid tumor using CLSM (Fig. 8B). As a result, no significant signals in heart and left and right lung were detected, suggesting that the HAL-LNP had some degree of selectivity for MPM tumors. However, the enhancement of *in vivo* cellular uptake was not drastic as well as *in vitro* experiment. This discrepancy might be attributed to an active production of HA by MPM cells.[25] Relatively higher concentration of HA in the pleural cavity might inhibit the cellular uptake of HAL-LNP.

Finally, we assessed the therapeutic effect of the system by loading the HAL-LNP with CDDP. The CDDP-loaded HAL-LNP was intrapleurally administered into the cavity at a CDDP dosage of 1.5 mg/kg at 7, 14, 21, 28 days after

the inoculation. In mice treated with PBS (−), MPM progressed not only on the ventral side but also on the dorsal side of lung and the pleural cavity (Fig. 9). Concerning free CDDP, MPM progressed in the pleural cavity to a smaller extent than PBS (−) (Average survival of CDDP and PBS (−) was 26.0 days and 36.5 days, respectively). On the other hand, the injection of the CDDP-loaded HAL-LNP substantially suppressed the progression of MPM (All mice survived 45 days after the injection). No evidence of solid tumor tissue was observed either in the dorsal side or the ventral side. These observations suggest that the HAL-modified LNP efficiently delivered therapeutics to MPM cells. Other groups have also developed nanoparticles for MPM therapy. For example, Ando *et al.* developed a cationic NNP without cholesterol and reported that it was an efficacious therapy for MPM.[48,49] In other cases, Kinoh *et al.*, reported that micelles releasing drugs that are responsive to acidification encapsulating staurosporine and epirubicin exhibited a marked therapeutic effect in an MPM model.[48] Accordingly, nanoparticles-based therapy appeared to be potent. In the near future, nanoparticle-based chemotherapy might be used in the therapeutic treatment of MPM patients.

4. Conclusion

We report herein on the design of a HA-conjugated lipid derivative (HAL) and show that the use of a combination of HAL and a cationic lipid nanoparticle (LNP) resulted in a selective, synergistic cellular uptake by CD44-positive malignant pleural mesothelioma (MPM) cells. An LNP containing 10 mol% of a cationic lipid modified with 2.0 mol% HAL was found to have the highest ability to target MPM cells. The optimized HAL-LNP encapsulating cis-diamminedichloro-platinum(II) (CDDP) achieved successful therapy for MPM-bearing mice.

5. Acknowledgement

The authors wish to thank Dr. Milton S Feather for appropriately modifying the manuscript. This study was supported, in part, by Ministry of Health, Labour and Welfare, by Ministry of Education, Culture, Sports, Science and Technology, by Japan Society for the Promotion of Science KAKENHI (Grant No. 18K18351) and by The Mochida Memorial Foundation for Medical and Pharmaceutical Research.

6. Table

Table 1 Characterization of DOTAP-containing LNPs.

DOTAP (mol%)	Sample	Diameter (nm)	Z-potential (mV)
0	LNP	144.1 ± 2.6	-8.5 ± 3.2
	HA + LNP	138.3 ± 0.4	-15.1 ± 2.8
	HAL-LNP	151.5 ± 1.0	-31.9 ± 0.4
5	LNP	119.7 ± 0.8	27.5 ± 3.0
	HAL-LNP	139.0 ± 1.8	-28.4 ± 2.2
10	LNP	123.2 ± 2.0	34.4 ± 1.6
	HA + LNP	129.0 ± 1.4	-28.8 ± 1.0
	HAL-LNP	141.3 ± 1.5	-29.2 ± 3.4
15	LNP	128.4 ± 1.8	37.8 ± 1.0
	HA + LNP	163.0 ± 4.2	-29.0 ± 0.3
	HAL-LNP	155.0 ± 0.3	-30.2 ± 1.9

Lipid composition: DSPC/chol/DOTAP, 50-x/50/x (molar ratio), Data indicates mean ± standard deviation (n=3)

7. Figure legends

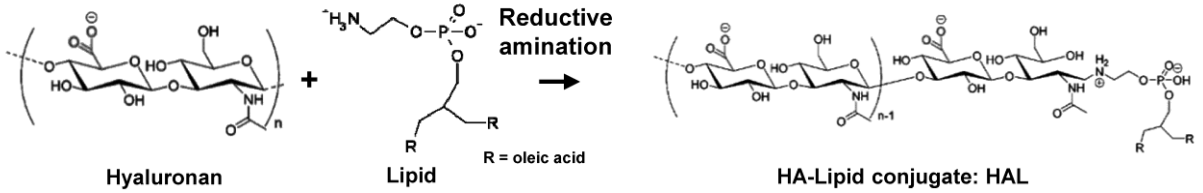

Figure 1. Schematic diagram showing the synthesis of HA-conjugated lipid derivatives (HAL). To display HA on the surface of the LNP, HA was conjugated with lipid by reductive amination.

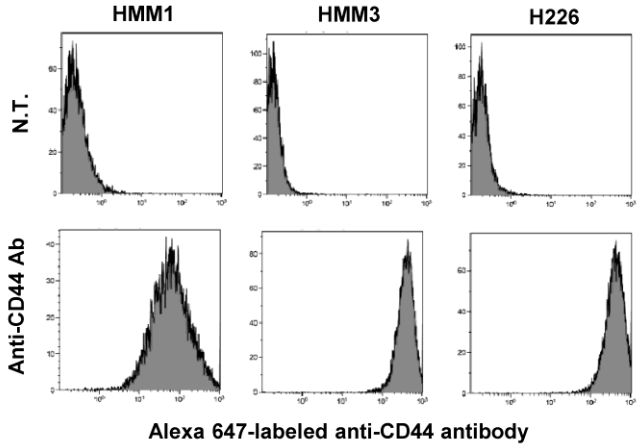

Figure 2. The expression level of the HA receptor CD44 in HMM1, HMM3 and H226 cells. The expression of the HA receptor CD44 was examined by flow cytometry. Upper panels show un-treated control. Lower panels indicate cells treated with Alexa 647-labeled anti-CD44 antibody in HMM1 (left), HMM3 (middle) and H226 (right).

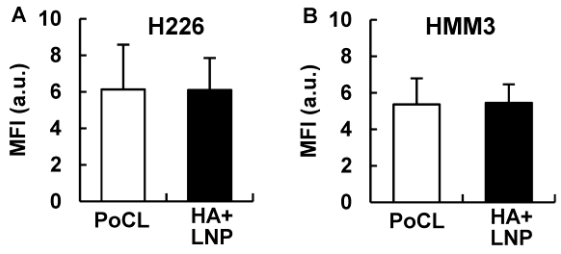

Figure 3. Failure of the cellular uptake of the HA-decorated LNP. The cellular uptake of HA-decorated cationic LNP in H226 and HMM3 was evaluated by flow cytometry. Fluorescent LNPs were added to cells and the cells were then subjected to flow cytometry analysis 2 hours after the addition. Y-axis indicates the mean fluorescent intensity (MFI). Bars indicate the mean ± standard deviation (SD) (n=3).

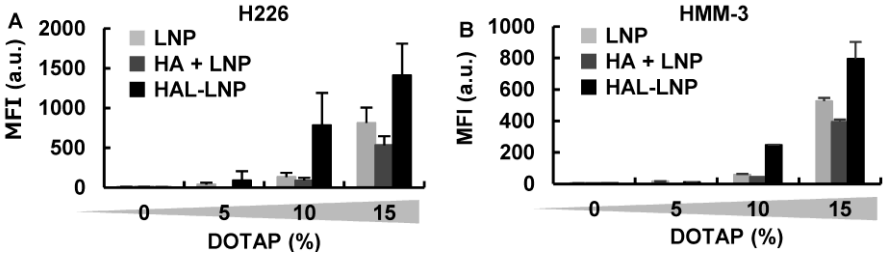

Figure 4. The synergistic effect on the cellular uptake of HAL and cationic LNP. The cellular uptake of the HAL-modified LNP was systematically analyzed by flow cytometry. When a conventional cationic lipid, DOTAP, was incorporated into LNPs at 0~10 mol% of the total lipid, the LNP was non-modified or modified with HA and HAL at 0.5 mol% of total lipid. The fluorescence intensity in cells was determined 2 hours after the addition of LNPs. Bars indicate the mean ± SD (n=3).

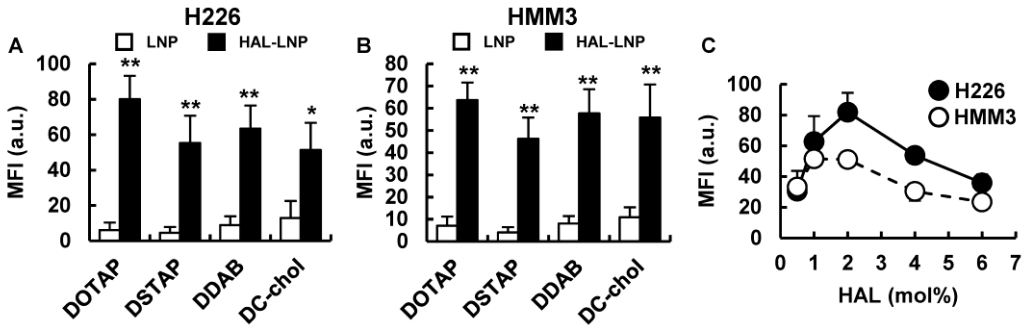

Figure 5. Optimization of HAL-LNP. A) Four LNPs containing different cationic lipids (DOTAP, DSTAP, DDAB and DC-chol) were evaluated in terms of cellular uptake by H226 and HMM3 cells. Bars indicate the mean ± SD (n=3). B) When the density of HAL was varied from 0.5 to 6.0 mol%, cellular uptake in H226 and HMM3 was evaluated by flow cytometry. Data indicate the mean ± SD (n=3).

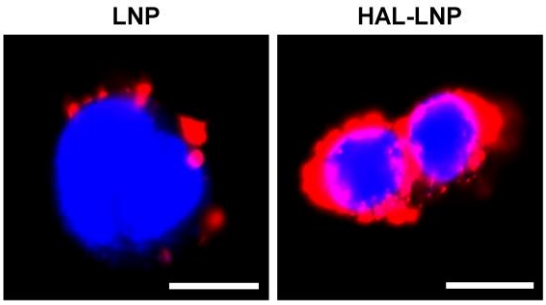

Figure 6. Intracellular localization of HAL-LNP. Cells were treated with DiI-labeled HAL-LNP and observed by CLSM. Blue and red dots indicate Hoechst33342 (nucleus) and DiI (HAL-LNP), respectively. Scale bars indicate 25 μm.

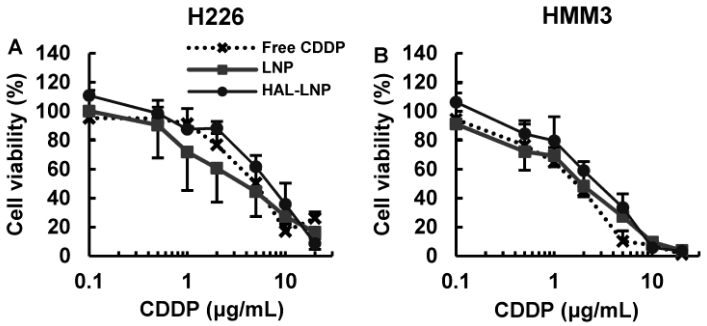

Figure 7. Cytotoxic effect by CDDP-loading HAL-LNP. CDDP was encapsulated into LNPs by the lipid thin layer method. Amount of CDDP encapsulated was determined by ICP-AES. Cell viability were determined by a WST-8 assay at 24 hours after the addition of CDDP at the indicated dosages (0.1 ~ 20 μg/mL). Data indicate the mean ± SD (n=3).

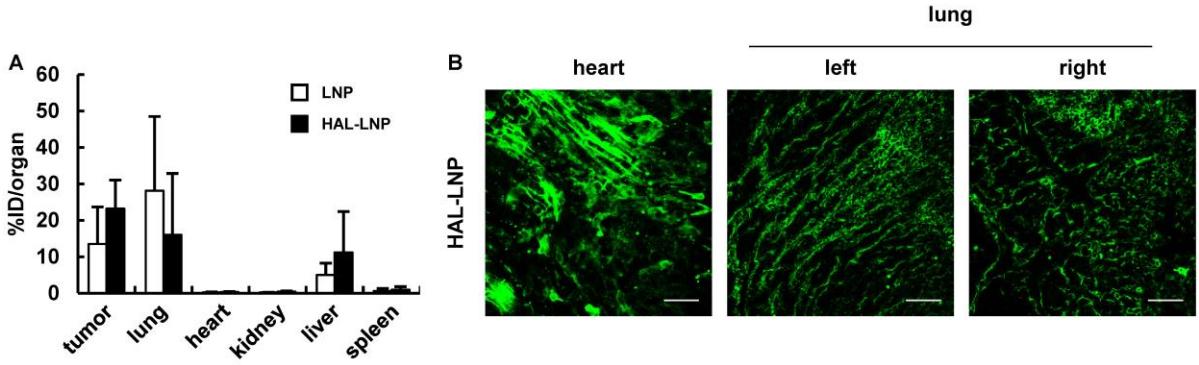

Figure 8. In vivo distribution of HAL-LNP after intrapleural injection. A) The distribution of LNP and HAL-LNP 24 hours after intrapleural injection was determined. Radioactivity derived from LNPs in tumor, lung, heart, kidney, liver and spleen tissue was detected by liquid scintillation counting. White and black columns indicate LNP and HAL-LNP, respectively. Bars indicate mean ± SD (n=3~6). B) Heart and lungs were observed after the intrapleural injections of DiI-labeled HAL-LNP. Green and red dots indicate Alexa488-labeled CD31-antibody (vessels) and DiI (LNP), respectively. Scale bars indicate 100 μm.

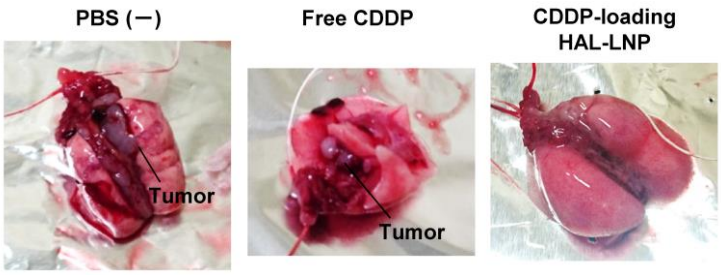

Figure 9. The therapeutic effect by CDDP-loading LNP against MPM-bearing mice. CDDP and CDDP-loading LNPs were intrapleurally administered a CDDP dosage of 1.5 mg/kg at 7, 14, 21 and 28 days using 2 independent mice after intrapleurally inoculating H226 cells into the cavity. At Day 45, lungs were excised and MPM progression was visually evaluated.

8. Conflict of Interest

The authors declared that there is no conflict of interest.

9. References

1. McDonald JC, McDonald AD 1996. The epidemiology of mesothelioma in historical context. Eur Respir J 9(9):1932-1942.

2. Chirieac LR, Barletta JA, Yeap BY, Richards WG, Tilleman T, Bueno R, Baldini EH, Godleski J, Sugarbaker DJ 2013. Clinicopathologic characteristics of malignant mesotheliomas arising in patients with a history of radiation for Hodgkin and non-Hodgkin lymphoma. J Clin Oncol 31(36):4544-4549.

3. Gibb H, Fulcher K, Nagarajan S, McCord S, Fallahian NA, Hoffman HJ, Haver C, Tolmachev S 2013. Analyses of radiation and mesothelioma in the US Transuranium and Uranium Registries. Am J Public Health 103(4):710-716.

4. Lin RT, Chang YY, Wang JD, Lee LJ 2018. Upcoming epidemic of asbestos-related malignant pleural mesothelioma in Taiwan: A prediction of incidence in the next 30 years. J Formos Med Assoc.

5. Curran D, Sahmoud T, Therasse P, van Meerbeeck J, Postmus PE, Giaccone G 1998. Prognostic factors in patients with pleural mesothelioma: the European Organization for Research and Treatment of Cancer experience. J Clin Oncol 16(1):145-152.

6. Kindler HL, Ismaila N, Armato SG, Bueno R, Hesdorffer M, Jahan T, Jones CM, Miettinen M, Pass H, Rimner A, Rusch V, Sterman D, Thomas A, Hassan R 2018. Treatment of Malignant Pleural Mesothelioma: American Society of Clinical Oncology Clinical Practice Guideline. J Clin Oncol 36(13):1343-1373.

7. Levin PA, Dowell JE 2017. Spotlight on bevacizumab and its potential in the treatment of malignant pleural mesothelioma: the evidence to date. Onco Targets Ther 10:2057-2066.

8. Ceresoli GL, Zucali PA, Mencoboni M, Botta M, Grossi F, Cortinovis D, Zilembo N, Ripa C, Tiseo M, Favaretto AG, Soto-Parra H, De Vincenzo F, Bruzzone A, Lorenzi E, Gianoncelli L, Ercoli B, Giordano L, Santoro A 2013. Phase II study of pemetrexed and carboplatin plus bevacizumab as first-line therapy in malignant pleural mesothelioma. Br J Cancer 109(3):552-558.

9. Fujimoto N, Aoe K, Kozuki T, Oze I, Kato K, Kishimoto T, Hotta K 2018. A Phase II Trial of First-Line Combination Chemotherapy With Cisplatin, Pemetrexed, and Nivolumab for Unresectable Malignant Pleural Mesothelioma: A Study Protocol. Clin Lung Cancer 19(5):e705-e707.

10. Mohamed H, Eltobgy M, Abdel-Rahman O 2017. Immune Checkpoints Aberrations and Malignant Mesothelioma: Assessment of Prognostic Value and Evaluation of Therapeutic Potentials. Anticancer Agents Med Chem 17(9):1228-1233.

11. Vogelzang NJ, Rusthoven JJ, Symanowski J, Denham C, Kaukel E, Ruffie P, Gatzemeier U, Boyer M, Emri S, Manegold C, Niyikiza C, Paoletti P 2003. Phase III study of pemetrexed in combination with cisplatin versus cisplatin alone in patients with malignant pleural mesothelioma. J Clin Oncol 21(14):2636-2644.

12. de Gooijer CJ, Baas P, Burgers JA 2018. Current chemotherapy strategies in malignant pleural mesothelioma. Transl Lung Cancer Res 7(5):574-583.

13. De Bondt C, Psallidas I, Van Schil PEY, van Meerbeeck JP 2018. Combined modality treatment in mesothelioma: a systemic literature review with treatment recommendations. Transl Lung Cancer Res 7(5):562-573.

14. Yamamoto S, Sakurai Y, Harashima H 2018. Failure of active targeting by a cholesterol-anchored ligand and improvement by altering the lipid composition to prevent ligand desorption. Int J Pharm 536(1):42-49.

15. Yamamoto S, Kato A, Sakurai Y, Hada T, Harashima H 2017. Modality of tumor endothelial VEGFR2 silencing-mediated improvement in intratumoral distribution of lipid nanoparticles. J Control Release 251:1-10.

16. Ara MN, Matsuda T, Hyodo M, Sakurai Y, Hatakeyama H, Ohga N, Hida K, Harashima H 2014. An aptamer ligand based liposomal nanocarrier system that targets tumor endothelial cells. Biomaterials 35(25):7110-7120.

17. Sakurai Y, Hatakeyama H, Sato Y, Hyodo M, Akita H, Ohga N, Hida K, Harashima H 2014. RNAi-mediated gene knockdown and anti-angiogenic therapy of RCCs using a cyclic RGD-modified liposomal-siRNA system. J Control Release 173:110-118.

18. Sakurai Y, Kajimoto K, Hatakeyama H, Harashima H 2015. Advances in an active and passive targeting to tumor and adipose tissues. Expert Opin Drug Deliv 12(1):41-52.

19. Hida K, Maishi N, Sakurai Y, Hida Y, Harashima H 2016. Heterogeneity of tumor endothelial cells and drug delivery. Adv Drug Deliv Rev 99(Pt B):140-147.

20. Sakurai Y, Hada T, Yamamoto S, Kato A, Mizumura W, Harashima H 2016. Remodeling of the Extracellular Matrix by Endothelial Cell-Targeting siRNA Improves the EPR-Based Delivery of 100 nm Particles. Mol Ther 24(12):2090-2099.

21. Lv Y, Xu C, Zhao X, Lin C, Yang X, Xin X, Zhang L, Qin C, Han X, Yang L, He W, Yin L 2018. Nanoplatform Assembled from a CD44-Targeted Prodrug and Smart Liposomes for Dual Targeting of Tumor Microenvironment and Cancer Cells. ACS Nano 12(2):1519-1536.

22. Lesley J, Hascall VC, Tammi M, Hyman R 2000. Hyaluronan binding by cell surface CD44. J Biol Chem 275(35):26967-26975.

23. Yang C, Cao M, Liu H, He Y, Xu J, Du Y, Liu Y, Wang W, Cui L, Hu J, Gao F 2012. The high and low molecular weight forms of hyaluronan have distinct effects on CD44 clustering. J Biol Chem 287(51):43094-43107.

24. Matsumura Y, Tarin D 1992. Significance of CD44 gene products for cancer diagnosis and disease evaluation. Lancet 340(8827):1053-1058.

25. Cortes-Dericks L, Schmid RA 2017. CD44 and its ligand hyaluronan as potential biomarkers in malignant pleural mesothelioma: evidence and perspectives. Respir Res 18(1):58.

26. Martensson G, Thylen A, Lindquist U, Hjerpe A 1994. The sensitivity of hyaluronan analysis of pleural fluid from patients with malignant mesothelioma and a comparison of different methods. Cancer 73(5):1406-1410.

27. Chono S, Li SD, Conwell CC, Huang L 2008. An efficient and low immunostimulatory nanoparticle formulation for systemic siRNA delivery to the tumor. J Control Release 131(1):64-69.

28. Maiolino S, Russo A, Pagliara V, Conte C, Ungaro F, Russo G, Quaglia F 2015. Biodegradable nanoparticles sequentially decorated with Polyethyleneimine and Hyaluronan for the targeted delivery of docetaxel to airway cancer cells. J Nanobiotechnology 13:29.

29. Ran R, Liu Y, Gao H, Kuang Q, Zhang Q, Tang J, Huang K, Chen X, Zhang Z, He Q 2014. Enhanced gene delivery efficiency of cationic liposomes coated with PEGylated hyaluronic acid for anti P-glycoprotein siRNA: a potential candidate for overcoming multi-drug resistance. Int J Pharm 477(1-2):590-600.

30. Surace C, Arpicco S, Dufaÿ-Wojcicki A, Marsaud V, Bouclier C, Clay D, Cattel L, Renoir JM, Fattal E 2009. Lipoplexes targeting the CD44 hyaluronic acid receptor for efficient transfection of breast cancer cells. Mol Pharm 6(4):1062-1073.

31. Landesman-Milo D, Goldsmith M, Leviatan Ben-Arye S, Witenberg B, Brown E, Leibovitch S, Azriel S, Tabak S, Morad V, Peer D 2013. Hyaluronan grafted lipid-based nanoparticles as RNAi carriers for cancer cells. Cancer Lett 334(2):221-227.

32. Cohen ZR, Ramishetti S, Peshes-Yaloz N, Goldsmith M, Wohl A, Zibly Z, Peer D 2015. Localized RNAi therapeutics of chemoresistant grade IV glioma using hyaluronan-grafted lipid-based nanoparticles. ACS Nano 9(2):1581-1591.

33. Banerji S, Wright AJ, Noble M, Mahoney DJ, Campbell ID, Day AJ, Jackson DG 2007. Structures of the Cd44-hyaluronan complex provide insight into a fundamental carbohydrate-protein interaction. Nat Struct Mol Biol 14(3):234-239.

34. Arpicco S, Lerda C, Dalla Pozza E, Costanzo C, Tsapis N, Stella B, Donadelli M, Dando I, Fattal E, Cattel L, Palmieri M 2013. Hyaluronic acid-coated liposomes for active targeting of gemcitabine. Eur J Pharm Biopharm 85(3 Pt A):373-380.

35. Goudarzi H, Iizasa H, Furuhashi M, Nakazawa S, Nakane R, Liang S, Hida Y, Yanagihara K, Kubo T, Nakagawa K, Kobayashi M, Irimura T, Hamada J 2013. Enhancement of in vitro cell motility and invasiveness of human malignant pleural mesothelioma cells through the HIF-1α-MUC1 pathway. Cancer Lett 339(1):82-92.

36. Goudarzi H, Hida Y, Takano H, Teramae H, Iizasa H, Hamada J 2013. Hypoxia affects in vitro growth of newly established cell lines from patients with malignant pleural mesothelioma. Biomed Res 34(1):13-21.

37. Martí Coma-Cros E, Biosca A, Lantero E, Manca ML, Caddeo C, Gutiérrez L, Ramírez M, Borgheti-Cardoso LN, Manconi M, Fernàndez-Busquets X 2018. Antimalarial Activity of Orally Administered Curcumin Incorporated in

Eudragit. Int J Mol Sci 19(5).

38. Mo L, Song JG, Lee H, Zhao M, Kim HY, Lee YJ, Ko HW, Han HK 2018. PEGylated hyaluronic acid-coated liposome for enhanced in vivo efficacy of sorafenib via active tumor cell targeting and prolonged systemic exposure. Nanomedicine 14(2):557-567.

39. Takara K, Hatakeyama H, Ohga N, Hida K, Harashima H 2010. Design of a dual-ligand system using a specific ligand and cell penetrating peptide, resulting in a synergistic effect on selectivity and cellular uptake. Int J Pharm 396(1-2):143-148.

40. Xia QS, Ding HM, Ma YQ 2017. Can dual-ligand targeting enhance cellular uptake of nanoparticles? Nanoscale 9(26):8982-8989.

41. van Haarst JM, Baas P, Manegold C, Schouwink JH, Burgers JA, de Bruin HG, Mooi WJ, van Klaveren RJ, de Jonge MJ, van Meerbeeck JP 2002. Multicentre phase II study of gemcitabine and cisplatin in malignant pleural mesothelioma. Br J Cancer 86(3):342-345.

42. Xiang Y, Liang L, Wang X, Wang J, Zhang X, Zhang Q 2011. Chloride channel-mediated brain glioma targeting of chlorotoxin-modified doxorubicine-loaded liposomes. J Control Release 152(3):402-410.

43. Hatakeyama H, Akita H, Harashima H 2013. The polyethyleneglycol dilemma: advantage and disadvantage of PEGylation of liposomes for systemic genes and nucleic acids delivery to tumors. Biol Pharm Bull 36(6):892-899.

44. Shmeeda H, Amitay Y, Gorin J, Tzemach D, Mak L, Ogorka J, Kumar S, Zhang JA, Gabizon A 2010. Delivery of zoledronic acid encapsulated in folate-targeted liposome results in potent in vitro cytotoxic activity on tumor cells. J Control Release 146(1):76-83.

45. Okabe K 2017. Intraoperative intracavitary hyperthermic chemotherapy for malignant pleural mesothelioma. Ann Transl Med 5(11):233.

46. Mujoomdar AA, Sugarbaker DJ 2008. Hyperthermic chemoperfusion for the treatment of malignant pleural mesothelioma. Semin Thorac Cardiovasc Surg 20(4):298-304.

47. Richards WG, Zellos L, Bueno R, Jaklitsch MT, Jänne PA, Chirieac LR, Yeap BY, Dekkers RJ, Hartigan PM, Capalbo L, Sugarbaker DJ 2006. Phase I to II study of pleurectomy/decortication and intraoperative intracavitary hyperthermic cisplatin lavage for mesothelioma. J Clin Oncol 24(10):1561-1567.

48. Kinoh H, Miura Y, Chida T, Liu X, Mizuno K, Fukushima S, Morodomi Y, Nishiyama N, Cabral H, Kataoka K 2016. Nanomedicines Eradicating Cancer Stem-like Cells in Vivo by pH-Triggered Intracellular Cooperative Action of Loaded Drugs. ACS Nano 10(6):5643-5655.

49. Ando H, Kobayashi S, Abu Lila AS, Eldin NE, Kato C, Shimizu T, Ukawa M, Kawazoe K, Ishida T 2015. Advanced therapeutic approach for the treatment of malignant pleural mesothelioma via the intrapleural administration of liposomal pemetrexed. J Control Release 220(Pt A):29-36.